

Achieving Reversible Sensing of Nitroxyl by Tuning the Ligand Environment of Azamacrocyclic Copper(II) Complexes

Sunghye Kim, Mikael A. Minier, Andrei Loas, Sabine Becker, Fang Wang, and Stephen J. Lippard*

Department of Chemistry, Massachusetts Institute of Technology, Cambridge, Massachusetts 02139, United States

S Supporting Information

ABSTRACT: To elucidate the factors that impart selectivity for nitroxyl (HNO) over nitric oxide (NO), thiols, and H₂S in metal-based fluorescent probes, we investigated five Cu(II)-cyclam (14-N₄) derivatives. Upon exposure to NO gas at pH 7, no changes occur in the UV–vis spectra of any of the complexes. Addition of Angeli's salt to generate HNO promotes reduction of Cu(II) only in the case of [Cu^{II}(14-N₄-Ts)(OTf)₂], which has the most positive reduction potential of the series. To gain insight into the observed reactivity, we prepared the Cu(II) complex of the mixed thia/aza 14-N₂S₂ ligand. [Cu^{II}(14-N₂S₂)(OTf)₂] reacts reversibly with HNO at pH 7, although nonselectively over thiols and H₂S. The recurrent sensing of HNO uncovered with the study of Cu(II) azamacrocyclic complexes is a remarkable feature that opens the door for the design of a new generation of metal-based probes.

Scientific interest in nitroxyl (HNO) was recently ignited by discoveries of its unique chemistry and biological properties.¹ Unlike nitric oxide (NO), exogenously applied HNO directly reacts with thiols,² activates the HNO-TRPA1-CGRP signaling cascade controlling cardiac contractility,³ and exerts therapeutic effects in the treatment of heart failure,⁴ cancer,¹ and alcoholism.⁵ Even though endogenous generation of HNO has not yet been demonstrated in vivo,^{1,4,6} several biosynthetic pathways to HNO have been elucidated in vitro. HNO is produced in cells by (i) neuronal nitric oxide synthase in the absence of the tetrahydrobiopterin cofactor,⁷ (ii) oxidation of hydroxylamine at the heme iron center of peroxidases, catalases, or myoglobin,⁸ and (iii) reduction of nitrite,⁹ NO,^{3,6b} and S-nitrosothiols.¹⁰ Given their orthogonal properties, the ability to discriminate between biological NO and HNO is critical for establishing their physiological functions. Direct, selective detection of HNO is currently accessible with amperometric¹¹ and fluorescent methods. Fluorescence bioimaging of HNO is the only technique that provides spatiotemporal resolution, achieved with reaction-¹² or metal-^{10,13} based probes. Among the latter, Cu(II)-based sensors for HNO operate by reduction of paramagnetic Cu(II) to diamagnetic Cu(I).^{13b} Cyclam (1,4,8,11-tetraazacyclotetradecane, 14-N₄) stands out as an excellent ligand for use in HNO sensors, owing to its tight Cu(II)-binding (pK_d ≈ 25)¹⁴ and low reactivity of Cu(II)-cyclam complexes with H₂S and thiols.¹⁵ Because of these properties, we previously designed the near-infrared-emitting CuDHX1^{13c} and the lysine-

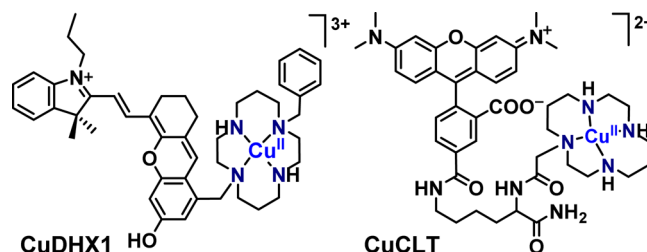


Figure 1. Structures of small-molecule fluorescent probes for HNO based on the Cu(II)-cyclam motif.

based CuCLT¹⁰ probes (Figure 1), which selectively detect HNO over other biological reductants.

Reversibility is a highly sought feature, because only reversible sensors are able to provide true spatiotemporal resolution¹⁶ and repeatedly detect sudden bursts of analyte production in vivo.¹⁷ Despite the advances (Figure 1), no reversible fluorescent probes for biological HNO are known.^{17,18} Modeling the metal-binding environment of existing sensors with synthetically accessible ligands is a promising strategy for achieving reversibility and establishing the features that provide selectivity toward HNO.

Accordingly, we investigated Cu(II)-cyclam analogues in which the nitrogen atoms of the macrocycle were systematically functionalized with methyl and tosyl (Ts) substituents. Following previously reported procedures,¹⁹ we prepared the 14-N₄-Me₂, 14-N₄-Me₃, 14-N₄-Me₄, and 14-N₄-Ts ligands (Figures 2 and S1–S5).

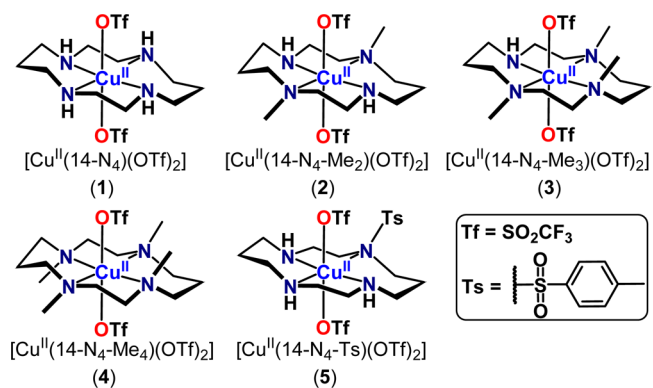


Figure 2. Structures and ligand abbreviations for Cu(II)-cyclam complexes produced in this work.

Received: December 8, 2015

Published: February 2, 2016

Table 1. Physical Properties of Copper(II) Azamacrocyclic Complexes

	1	2	3	4	5	6	solvent
d-d band λ_{max} , nm	507 (94)	518 (170)	568 (202)	560 (206)	549 (170)	556 (580)	buffer ^a (pH 7.0)
(ϵ , M ⁻¹ cm ⁻¹)	504 (84)	509 (148)	554 (189)	546 (199)	545 (182)	542 (557)	MeOH
Cu(II/I) $E_{1/2}$, V ^b	-1.25	-0.92	-0.83	-0.79	n.d. ^d	n.d. ^d	MeCN
Cu(II/I) E_{pc} , V ^c	-1.29	-0.99	-0.91	-0.86	-0.86	-0.74, -0.57	MeCN
EPR parameters							MeOH
g_{\parallel} =	2.253	2.250	2.256	2.258	2.242	2.221	
g_{\perp} =	1.979	1.983	1.994	1.995	2.006	2.005	
A_{\parallel} =	159 G	155 G	155 G	151 G	149 G	181 G	

^a50 mM PIPES, 100 mM KCl. ^b $E_{1/2}$, half-wave (redox) potential vs Fc⁺/Fc. ^c E_{pc} cathodic peak potential vs Fc⁺/Fc. ^dNot determined.

The Cu(II) complexes of these ligands as well as that of the 14-N₄ parent were isolated as triflate (OTf⁻) salts (1–5 in Figure 2) and characterized by X-ray diffraction, elemental analysis, cyclic voltammetry, and EPR and UV–vis spectroscopy (see Supporting Information (SI), Table 1, and Figures S6–S9). All complexes displayed weak ($\epsilon < 10^3$ M⁻¹ cm⁻¹) d–d electronic absorptions in the 500–560 nm range, characteristic of square planar Cu(II) species,²⁰ and axial Cu(II) EPR signals in methanol (Table 1). Coordination of OTf⁻ counterions to the Cu(II) centers produced distorted octahedral structures in the solid state, with the substituted cyclam rings adopting *trans*-III conformations^{20,21} (Tables S1–S3, and Figure S7).

With these Cu(II)-cyclam complexes in hand, we first evaluated their reactivity toward NO and HNO at physiological pH. Exposure of anaerobic solutions of 1–5 to excess NO(g) in pH 7 aqueous buffer did not produce any changes in their UV–vis spectra (shown for 5 in Figure S10b). Treatment of compounds 1–4 with 50 equiv of the HNO donor Angeli's salt (AS)²² also did not alter their UV–vis spectra. [Cu^{II}(14-N₄-Ts)(OTf)₂] (5), however, reacted readily with AS, as evidenced by a red-shift of the Cu(II) d–d band at 549 nm along with a decrease in its intensity and discoloration of the purple aqueous solution (Figure S10a). Similar results were obtained in methanol (Figure S11a). AS releases equimolar amounts of HNO and nitrite ion (NO₂⁻).²² Anaerobic treatment of 5 with 50 equiv of NaNO₂ at pH 7 did not elicit any changes in the d–d band of the complex (Figure S10g), confirming that nitrite is not the species responsible for the observed color change. We further investigated the fate of the copper ion by ESI-MS, NMR, and EPR spectroscopy. ESI-MS analyses of the reaction solutions of 5 with AS in both aqueous buffer and methanol revealed the demetallated 14-N₄-Ts ligand as the only detectable species (Figures S10h and S11b). The ¹H NMR spectrum of a mixture of 5 and 50 equiv of AS in CD₃OD was essentially the same as that of the metal-free ligand, further supporting the demetalation reaction (Figure S12). Upon anaerobic treatment of 5 with AS in methanol, a new axial EPR signal with significantly lower intensity emerged (Figure S13), suggesting partial reduction of Cu(II) and metal dissociation. The inability to reduce the Cu(II) probe fully to a Cu(I) species in the EPR tube was previously encountered in cyclam-based HNO sensors, with¹⁰ or without^{13c} metal retention in the binding site. No metal release was observed when 2 equiv of NaOH were added to both buffered and methanolic solutions of 5 (Figure S14), indicating that potential increases in pH upon addition of basic solutions of AS are not the cause of the observed demetalation.

We also attempted to structurally characterize the reduced form of 5. Efforts to isolate Cu^I(14-N₄-Ts) anaerobically, however, resulted in spontaneous disproportionation of the complex, reflecting the known lability of Cu(I)-cyclam analogues.^{21,23} Taken together, the foregoing results support

reduction of Cu(II) in 5 by HNO, followed by dissociation of Cu(I) from the ligand and formation of a new Cu(II) species with a weaker ligand field (lower energy d–d band)²⁰ as a result of reoxidation in solution.

To investigate the factors imparting reactivity toward HNO, we performed cyclic voltammetry studies on the complexes in acetonitrile using a three-electrode setup. An increase in the Cu(II/I) reduction potentials ($E_{1/2}$ or E_{pc} , Table 1) was observed as the number of electron-donating methyl groups increased, from -1.25 (in 1) to -0.79 (in 4) V vs Fc⁺/Fc. This seemingly counterintuitive trend can be explained by the relief of steric strain²⁴ caused by interactions of the cyclam methyl substituents and the Cu(II) axial ligands upon conversion from an octahedral Cu(II) to a tetrahedral Cu(I) geometry. The propensity of such steric factors to influence the redox behavior of copper-cyclam²⁵ and copper-diamine²⁶ complexes is well documented. The reductions of 3 and 4 remained chemically irreversible even at scan rates of 1 V s⁻¹. As for previously reported Cu^{II}(14-N₄-Me₄) analogues,²⁷ new redox couples appeared as a result of rapid isomerization of the initial Cu(I) *trans*-III conformation at the electrode surface (Figure S8). In the case of the Ts derivative 5, only the Cu(II) reduction event at $E_{\text{pc}} = -0.86$ V vs Fc⁺/Fc could be isolated.

It is noteworthy that, even though 4 and 5 have the most positive E_{pc} of the five Cu(II)-cyclam compounds (Figure S8), 5 is the only one of the series exhibiting reactivity toward HNO. Nitroxyl ($E_{\text{pc,NO/NO}^-} \approx -1.4$ V vs Fc⁺/Fc in acetonitrile)²⁸ is thermodynamically able to reduce all the complexes, whereas NO ($E_{\text{pc,NO}^+/\text{NO}} \approx +0.8$ V vs Fc⁺/Fc in acetonitrile)²⁹ cannot reduce any. At pH 7, however, the irreversible proton-coupled reduction of NO to HNO is expected to occur at potential values between -0.8 and -0.14 V vs NHE,^{5,6b,28} but the thermodynamic potential of the NO, H⁺/HNO couple is not known. These observations indicate that favorable electronic factors are not always sufficient for evoking the desired reactivity, and that the steric parameters of the ligand environment are key to facilitating reduction of Cu(II) by HNO. We expected that the more positive E_{pc} of 5 would allow for reaction with weaker reductants than HNO. Indeed, excess cysteine (Cys), glutathione (GSH), and H₂S ($E_{1/2} \approx -0.3$ V vs NHE at pH 7)³⁰ added under N₂ to pH 7 buffered aqueous solutions of 5 led to the disappearance of the Cu(II) d–d band (Figure S10), consistent with the reported stabilization of Cu(I)-thiolate complexes in anaerobic solutions.³¹

Considering that dissociation of Cu(I) from the 14-N₄-Ts ligand prevents reversible binding of HNO in 5, we introduced soft S-donor atoms to facilitate the desired chemistry by stabilizing a tetrahedral Cu(I) unit in the macrocyclic binding pocket.³² The Cu(II) complex of 1,8-dithia-4,11-diazacyclotetradecane (14-N₂S₂)³³ was prepared by treatment of 14-N₂S₂ with Cu(OTf)₂ in acetone, followed by vapor diffusion of diethyl

ether to yield purple X-ray-quality crystals of $[\text{Cu}^{\text{II}}(14\text{-N}_2\text{S}_2)(\text{OTf})_2]$ (**6**). The crystal structure of **6** revealed the expected coordination of two OTf⁻ ligands to the square planar Cu(II) center (Figure 3a), affording an octahedral geometry similar to

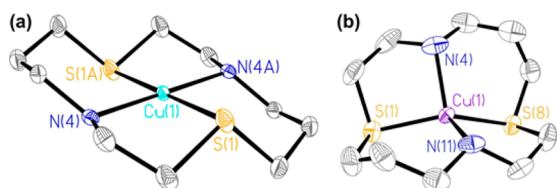


Figure 3. X-ray structures of (a) $[\text{Cu}^{\text{II}}(14\text{-N}_2\text{S}_2)(\text{OTf})_2]$ (**6**) and (b) $[\text{Cu}^{\text{I}}(14\text{-N}_2\text{S}_2)](\text{PF}_6)$ (**7**) in ORTEP representations at 50% probability. H atoms, axial OTf⁻ ligands, and PF₆⁻ counterions were omitted for clarity (see Figure S7).

that in compounds **1–5** (Tables S1–S3, Figure S7). The EPR spectrum of **6** displayed the usual Cu(II) axial signal (Table 1, Figure S6). In addition, we isolated and characterized colorless crystals of $[\text{Cu}^{\text{I}}(14\text{-N}_2\text{S}_2)](\text{PF}_6)$ (**7**) from the reaction of 14-N₂S₂ with $[\text{Cu}(\text{CH}_3\text{CN})_4](\text{PF}_6)$ under nitrogen. The X-ray structure of **7** (Figures 3b and S7f) revealed a highly distorted Cu(I) tetrahedral geometry.

Mixed thia/aza donor ligands shift the reduction potentials of coordinated metals to values higher than those of the aza-only analogues.^{14,25,32} Accordingly, the cyclic voltammogram of **6** in acetonitrile exhibited the most positive Cu(II/I) E_{pc} among all complexes **1–6**. Two irreversible reduction waves were observed for **6**, at $E_{\text{pc}} = -0.74$ and -0.57 V vs Fc^{+/0}, together with two chemically uncoupled oxidation events (Figure S9). This redox behavior can be attributed to new copper species formed by coordination of CH₃CN or, as in the case of **5**, rapid conformational isomerization of the macrocyclic ligand.²⁷ As is the case for **1–5**, no reaction occurred when **6** was exposed to excess NO(g) (Figure S18a). Addition of only 10 equiv of AS to an anaerobic aqueous solution of **6** at pH 7, however, produced an immediate loss of the Cu(II) d–d band at 556 nm (Figure 4), indicating reduction to a Cu(I) species.

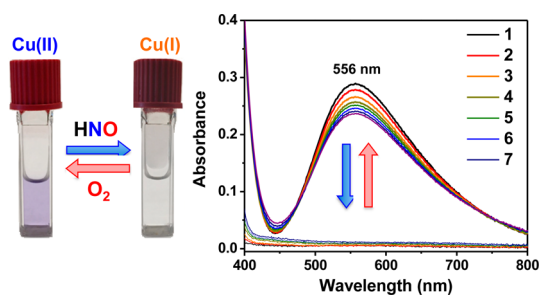
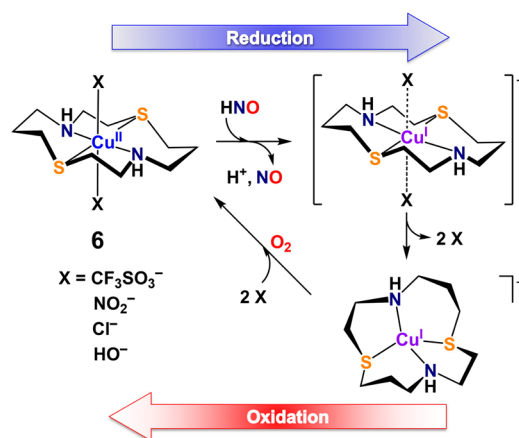


Figure 4. UV–vis spectra of an anaerobic 0.5 mM solution of **6** in aqueous buffer, acquired upon successive additions of 10 equiv of AS to the reoxidized complex (25 °C, 100 mM KCl, 50 mM PIPES, pH 7.0).

Importantly, the d–d band and the purple color of the Cu(II) complex were regenerated upon exposure to air or dioxygen for 10 min, indicating that reoxidation of Cu(I) had occurred. Further purging of the solution with N₂ and subsequent addition of 10 equiv of AS reproduced the loss of absorbance at 556 nm. We repeated the Cu(II)–Cu(I) interconversion seven times and observed <20% decrease of the initial d–d band absorbance (Figure 4). The reduction of **6** by HNO and regeneration of the Cu(II) form also occur in air or with 5% O₂ added to the

anaerobic cuvette to simulate tissue normoxia (Figure S16). No reaction or metal dissociation was observed when a pH 7 buffered solution of **6** was treated with NaOH alone (Figure S17a). The reversible redox chemistry at the copper center upon consecutive cycles of oxygenation and treatment with AS, respectively, demonstrates the ability of **6** to continually respond to steady fluxes of HNO at physiological pH and O₂ levels. Similar results were obtained in the presence of 100 equiv of NaNO₂, indicating that the nitrite ion, a byproduct of AS decomposition,²² does not interfere with the reversible transformation (Figure S19). ESI-MS analysis of the aqueous reaction solution following reduction by HNO revealed Cu-bound **6** to be the major species (Figure S15b), confirming retention of the metal ion in the thia/aza binding site. The formation of the $[\text{Cu}^{\text{I}}(14\text{-N}_2\text{S}_2)]^+$ cation was further supported by the ¹H NMR spectrum of a mixture of **6** and 10 equiv of AS in anaerobic CD₃OD, which was identical to that of the authentic Cu(I) complex **7** (Figure S20). To the best of our knowledge, **6** offers the first example of reversible HNO sensing in aqueous solution by a Cu(II) complex, the reactivity of which is summarized in Scheme 1.

Scheme 1. Reactivity Cycle of **6** with HNO



From thermodynamic considerations (see the discussion above for **5**), NO produced in the reaction of **6** with HNO (Scheme 1) cannot reoxidize the complex on its own. The UV–vis spectrum of an AS-treated anaerobic solution of **6** remains spectroscopically silent even after exposure to excess NO(g) for 30 min (Figure S22). Also, NO(g) did not alter the UV–vis spectrum of the Cu(I) analogue **7** (Figure S23). We also investigated the effect of pH on the reactivity of **6** with HNO. Between pH 7 and 9, **6** is reversibly reduced by HNO. At pH 10, **6** reacts with HNO with limited reversibility, the Cu(II) d–d band being restored to less than half its original intensity after three cycles (Figure S21a). At pH 12, **6** is irreversibly reduced by HNO, and at pH 14, deprotonation of the N-donors²⁰ leads to release of Cu(II) in solution (Figure S21b,c). ESI-MS spectra of these solutions revealed partial N-nitrosation and S-oxidation of the ligand following reaction with HNO (Figure S21). Metal dissociation was also observed in a basic solution of **6** in methanol (Figure S17b). These results demonstrate that the metal- and proton-binding properties of **6** are optimal for repeatedly detecting HNO at pH 7. Increases in pH lead to metal release in solution, abolishing reversibility. Despite its desirable features, the more positive Cu(II/I) E_{pc} of **6** makes it prone to reduction by other biological species. In particular, Cys, GSH,

and H₂S(g) irreversibly reduce the complex (Figure S18) with attendant metal dissociation.

In summary, the present investigation has significantly enhanced our understanding of the electronic and structural factors that determine the reactivity of Cu(II)-based azamacrocyclic complexes with nitroxyl. Lower Cu(II/I) redox potentials promote selectivity for HNO over other biological reductants. Reduction of Cu(II), however, is accompanied by structural changes and occurs only when promoted by geometric features of the binding site. The ability of the ligand to accommodate and stabilize the tetrahedral Cu(I) center is critical for attaining reversibility in aqueous solution. The recurrent binding of HNO discovered with [Cu^{II}(14-N₂S₂)(OTf)₂] (6) is a significant advance toward detecting this elusive chemical messenger in biology. Further ligand optimization is currently ongoing to achieve HNO selectivity and to incorporate these features in fluorescent sensors for imaging HNO in vivo.

■ ASSOCIATED CONTENT

Supporting Information

The Supporting Information is available free of charge on the ACS Publications website at DOI: 10.1021/jacs.5b12825.

Materials and methods, experimental details, NMR and ESI-MS spectra, X-ray crystallographic data, EPR and UV-vis spectra, cyclic voltammetry, and reactivity studies, including Figures S1–S23 and Tables S1–S3 (PDF)

■ AUTHOR INFORMATION

Corresponding Author

*lippard@mit.edu

Notes

The authors declare no competing financial interest.

■ ACKNOWLEDGMENTS

This work was supported by the National Science Foundation under grant CHE-1265770. We thank Dr. Alexandria Deliz Liang for assistance with EPR spectroscopy.

■ REFERENCES

- (1) Switzer, C. H.; Flores-Santana, W.; Mancardi, D.; Donzelli, S.; Basudhar, D.; Ridnour, L. A.; Miranda, K. M.; Fukuto, J. M.; Paolucci, N.; Wink, D. A. *Biochim. Biophys. Acta, Bioenerg.* **2009**, *1787*, 835–840.
- (2) Miranda, K. M. *Coord. Chem. Rev.* **2005**, *249*, 433–455.
- (3) Eberhardt, M.; Dux, M.; Namer, B.; Miljkovic, J.; Cordasic, N.; Will, C.; Kichko, T. I.; de la Roche, J.; Fischer, M.; Suarez, S. A.; Bikiel, D.; Dorsch, K.; Leffler, A.; Babes, A.; Lampert, A.; Lennerz, J. K.; Jacobi, J.; Marti, M. A.; Doctorovich, F.; Hogestatt, E. D.; Zygmunt, P. M.; Ivanovic-Burmazovic, I.; Messlinger, K.; Reeh, P.; Filipovic, M. R. *Nat. Commun.* **2014**, *5*, 4381.
- (4) Bullen, M. L.; Miller, A. A.; Andrews, K. L.; Irvine, J. C.; Ritchie, R. H.; Sobey, C. G.; Kemp-Harper, B. K. *Antioxid. Redox Signaling* **2011**, *14*, 1675–1686.
- (5) Flores-Santana, W.; Salmon, D. J.; Donzelli, S.; Switzer, C. H.; Basudhar, D.; Ridnour, L.; Cheng, R.; Glynn, S. A.; Paolucci, N.; Fukuto, J. M.; Miranda, K. M.; Wink, D. A. *Antioxid. Redox Signaling* **2011**, *14*, 1659–1674.
- (6) (a) Fukuto, J. M.; Cisneros, C. J.; Kinkade, R. L. *J. Inorg. Biochem.* **2013**, *118*, 201–208. (b) Suarez, S. A.; Neuman, N. I.; Muñoz, M.; Álvarez, L.; Bikiel, D. E.; Brondino, C. D.; Ivanović-Burmazović, I.; Miljkovic, J. L.; Filipovic, M. R.; Marti, M. A.; Doctorovich, F. *J. Am. Chem. Soc.* **2015**, *137*, 4720–4727.
- (7) Adak, S.; Wang, Q.; Stuehr, D. J. *J. Biol. Chem.* **2000**, *275*, 33554–33561.
- (8) Donzelli, S.; Espey, M. G.; Flores-Santana, W.; Switzer, C. H.; Yeh, G. C.; Huang, J. M.; Stuehr, D. J.; King, S. B.; Miranda, K. M.; Wink, D. A. *Free Radical Biol. Med.* **2008**, *45*, 578–584.
- (9) Miljkovic, J. L.; Kenkel, I.; Ivanovic-Burmazovic, I.; Filipovic, M. R. *Angew. Chem., Int. Ed.* **2013**, *52*, 12061–12064.
- (10) Loas, A.; Radford, R. J.; Liang, A. D.; Lippard, S. J. *Chem. Sci.* **2015**, *6*, 4131–4140.
- (11) Suarez, S. A.; Bikiel, D. E.; Wetzler, D. E.; Marti, M. A.; Doctorovich, F. *Anal. Chem.* **2013**, *85*, 10262–10269.
- (12) (a) Kawai, K.; Ieda, N.; Aizawa, K.; Suzuki, T.; Miyata, N.; Nakagawa, H. *J. Am. Chem. Soc.* **2013**, *135*, 12690–12696. (b) Jing, X.; Yu, F.; Chen, L. *Chem. Commun.* **2014**, *50*, 14253–14256. (c) Miao, Z. R.; Reisz, J. A.; Mitroka, S. M.; Pan, J.; Xian, M.; King, S. B. *Bioorg. Med. Chem. Lett.* **2015**, *25*, 16–19.
- (13) (a) Marti, M. A.; Bari, S. E.; Estrin, D. A.; Doctorovich, F. *J. Am. Chem. Soc.* **2005**, *127*, 4680–4684. (b) Rosenthal, J.; Lippard, S. J. *J. Am. Chem. Soc.* **2010**, *132*, 5536–5537. (c) Wrobel, A. T.; Johnstone, T. C.; Liang, A. D.; Lippard, S. J.; Rivera-Fuentes, P. *J. Am. Chem. Soc.* **2014**, *136*, 4697–4705.
- (14) Ambundo, E. A.; Deydier, M. V.; Grall, A. J.; Aguera-Vega, N.; Dressel, L. T.; Cooper, T. H.; Heeg, M. J.; Ochrymowycz, L. A.; Rorabacher, D. B. *Inorg. Chem.* **1999**, *38*, 4233–4242.
- (15) Sasakura, K.; Hanaoka, K.; Shibuya, N.; Mikami, Y.; Kimura, Y.; Komatsu, T.; Ueno, T.; Terai, T.; Kimura, H.; Nagano, T. *J. Am. Chem. Soc.* **2011**, *133*, 18003–18005.
- (16) Tonzetich, Z. J.; McQuade, L. E.; Lippard, S. J. *Inorg. Chem.* **2010**, *49*, 6338–6348.
- (17) Kaur, A.; Kolanowski, J. L.; New, E. J. *Angew. Chem., Int. Ed.* **2016**, *55*, 1602–1613.
- (18) Li, X.; Gao, X.; Shi, W.; Ma, H. *Chem. Rev.* **2014**, *114*, 590–659.
- (19) (a) Royal, G.; Dahaoui-Gindrey, V.; Dahaoui, S.; Tabard, A.; Guillard, R.; Pullumbi, P.; Lecomte, C. *Eur. J. Org. Chem.* **1998**, *1998*, 1971–1975. (b) Halfen, J. A.; Young, V. G., Jr. *Chem. Commun.* **2003**, 2894–2895. (c) Yang, W.; Giandomenico, C. M.; Sartori, M.; Moore, D. A. *Tetrahedron Lett.* **2003**, *44*, 2481–2483.
- (20) Goeta, A. E.; Howard, J. A. K.; Maffeo, D.; Puschmann, H.; Williams, J. A. G.; Yufit, D. S. *J. Chem. Soc., Dalton Trans.* **2000**, 1873–1880.
- (21) Amatore, C.; Barbe, J.-M.; Bucher, C.; Duval, E.; Guillard, R.; Verpeaux, J.-N. *Inorg. Chim. Acta* **2003**, *356*, 267–278.
- (22) Miranda, K. M.; Dutton, A. S.; Ridnour, L. A.; Foreman, C. A.; Ford, E.; Paolucci, N.; Katori, T.; Tocchetti, C. G.; Mancardi, D.; Thomas, D. D.; Espey, M. G.; Houk, K. N.; Fukuto, J. M.; Wink, D. A. *J. Am. Chem. Soc.* **2005**, *127*, 722–731.
- (23) Hoppe, T.; Schaub, S.; Becker, J.; Würtele, C.; Schindler, S. *Angew. Chem., Int. Ed.* **2013**, *52*, 870–873.
- (24) Ciampolini, M.; Fabbrizzi, L.; Licchelli, M.; Perotti, A.; Pezzini, F.; Poggi, A. *Inorg. Chem.* **1986**, *25*, 4131–4135.
- (25) Comba, P.; Jakob, H. *Helv. Chim. Acta* **1997**, *80*, 1983–1991.
- (26) Citek, C.; Lin, B. L.; Phelps, T. E.; Wasinger, E. C.; Stack, T. D. P. *J. Am. Chem. Soc.* **2014**, *136*, 14405–14408.
- (27) Bucher, C.; Duval, E.; Espinosa, E.; Barbe, J.-M.; Verpeaux, J.-N.; Amatore, C.; Guillard, R. *Eur. J. Inorg. Chem.* **2001**, *2001*, 1077–1079.
- (28) Bartberger, M. D.; Liu, W.; Ford, E.; Miranda, K. M.; Switzer, C.; Fukuto, J. M.; Farmer, P. J.; Wink, D. A.; Houk, K. N. *Proc. Natl. Acad. Sci. U. S. A.* **2002**, *99*, 10958–10963.
- (29) Lee, K. Y.; Kuchynka, D. J.; Kochi, J. K. *Inorg. Chem.* **1990**, *29*, 4196–4204.
- (30) Alberty, R. A. *Biophys. Chem.* **2004**, *111*, 115–122.
- (31) Rigo, A.; Corazza, A.; di Paolo, M. L.; Rossetto, M.; Ugolini, R.; Scarpa, M. *J. Inorg. Biochem.* **2004**, *98*, 1495–1501.
- (32) Bernardo, M. M.; Heeg, M. J.; Schroeder, R. R.; Ochrymowycz, L. A.; Rorabacher, D. B. *Inorg. Chem.* **1992**, *31*, 191–198.
- (33) Walker, T. L.; Malasi, W.; Bhide, S.; Parker, T.; Zhang, D.; Freedman, A.; Modarelli, J. M.; Engle, J. T.; Ziegler, C. J.; Custer, P.; Youngs, W. J.; Taschner, M. J. *Tetrahedron Lett.* **2012**, *53*, 6548–6551.